IEEE Access
Multidisciplinary : Rapid Review : Open Access Journal

Received 8 June 2023, accepted 26 June 2023, date of publication 30 June 2023, date of current version 7 July 2023.
Digital Object Identifier 10.1109/ACCESS.2023.3290992

RESEARCH ARTICLE

Cooperative Transit Signal Priority Considering Bus Stops Under Adaptive Signal Control

CHANGLONG ZHANG[1], XIAODONG YANG[1], JIMIN WEI[1], SHUO YANG[2], JINGANG DAI[1], AND SHIBO QU[1]
[1]Changsha Intelligent Driving Institute Company Ltd., Changsha 410208, China
[2]Liuzhou Dongke Smart City Investment and Development Company Ltd., Liuzhou 545001, China
Corresponding author: Jimin Wei (wei.jm@cidi.ai)

ABSTRACT Cooperative transit signal priority (CTSP), which integrates cellular vehicle-to-everything (C-V2X) technology, can improve the efficiency of connected transit vehicles at signalized intersections. However, few studies have considered the impact of bus stops on CTSP under adaptive signal control. Near-side bus stops at an intersection and multiple transit vehicles arriving at the same bus stop affect the bus arrival prediction. To overcome these shortcomings, we propose a Cooperative Transit signal priority method under Adaptive signal control considering bus Stops (CTAS). The queue prediction model is built with the real-time traffic data from the roadside perception system at intersections. The distance prediction model is built with real-time transit vehicles data, queue length, location of the bus stop, dwell time, and the preceding transit vehicles at the bus stop. Then the optimal signal timing plan is obtained by minimizing the total person delay. Finally, the rolling horizon strategy is utilized to continuously adjust the signal timing plan to adapt to changing traffic conditions. We verify the proposed method using measured data from an intersection in Changsha. The results indicate that our method achieves the best performance in terms of bus delay and person delay compared with the existing methods. It is an effective method to improve efficiency for transit vehicles and passengers.

INDEX TERMS Adaptive signal control, bus stops, C-V2X, cooperative transit signal priority, person delay.

I. INTRODUCTION

Transit signal priority (TSP) is a strategy that can reduce travel times for transit vehicles at signalized intersections [1], [2] and relieve traffic congestion [3], [4]. Conventional TSP strategies include green time extension [5], [6], red time truncation [7], [8], green time insertion [9], and cycle extension [10]. However, it is challenging to obtain real-time accurate data on transit vehicles in conventional methods, because transit vehicles are detected by stationary sensors(e.g., loop detectors, cameras, or RFID detectors). Inaccurate data can lead to a waste of extra green time and cause adverse effects [7], [11].

In recent years, cellular vehicle-to-everything (C-V2X) technology has benefited signal control systems by providing real-time accurate vehicle data (position, velocity, heading, occupancy, etc.) via the vehicle-to-infrastructure (V2I) communication [12], [13], [14]. Cooperative transit signal priority (CTSP) [15] and signal preemption [16] are enabled with this technology. CTSP outperforms conventional TSP in terms of reducing bus delay and person delay [11], [17], [18]. Furthermore, CTSP can effectively reduce negative impacts on private vehicles in conflicting directions when providing priority for transit vehicles [7], [17], [19], [20]. CTSP requires the status data on both queueing vehicles and approaching vehicles at intersections. These data are used to optimize the performance criteria such as transit vehicle delay [17], person delay [19], [20], [21], or queue length [7]. Therefore, a high penetration rate of connected vehicles is necessary to obtain sufficient vehicle status data for these studies. However, the penetration rate of connected vehicles is still very low at present and is expected to reach 40%∼62% in 2030 [22]. This makes these methods inapplicable under existing conditions.

CTSP has been achieved in many studies under the condition that only transit vehicles are connected vehicles [11] due to the low penetration rate of connected vehicles. These

The associate editor coordinating the review of this manuscript and approving it for publication was Maurice J. Khabbaz.

studies can be classified into two categories: CTSP under fixed-time signal control and CTSP under adaptive signal control. The majority of these studies focus on fixed-time signal control and provide priority for transit vehicles by adjusting the fixed signal timing [15], [18], [23], [24], [25]. Zeng et al. proposed a localized transit signal priority (L-TSP) model aiming to respond to priority requests of transit vehicles without causing major changes to the original signal timing plan [23], [24]. Hu et al. introduced a green time reallocation method, which can address multiple conflicting priority requests at an isolated intersection [18]. Although these studies can reduce the negative impacts on the other vehicles during the implementation of CTSP, they can only adjust the signal timing plan when a transit vehicle arrives.

Adaptive signal control can adjust traffic signal timing plan according to real-time traffic status, but it is unable to provide preferential treatment to transit vehicles [26], [27]. The current CTSP methods under fixed-time signal control are not suitable for adaptive signal control environment because the traffic signal timing plan constantly changes according to the traffic status. Therefore, it is significant to integrate CTSP and adaptive signal control when only transit vehicles are connected vehicles. There is a little research about CTSP under adaptive signal control at present. Lee et al. proposed a Person-based Adaptive traffic signal control method with Cooperative Transit signal priority (PACT), which obtains the real-time information of non-connected vehicles with a roadside perception system and achieves CTSP by minimizing the total person delay [27], [28]. However, this method does not consider bus stops, which are commonly located near intersections. The effectiveness of TSP relies on accurate arrival prediction for transit vehicles [5], [17]. The impact of bus stops should be considered based on the following reasons. (a)The dwell time of the transit vehicle at the bus stop is necessary for boarding and deboarding passengers. (b)When multiple transit vehicles approach the same bus stop, the subsequent transit vehicle may be blocked by the preceding ones and unable to enter the bus stop, which will increase the waiting time of the subsequent transit vehicle. These challenges lead to inaccurate arrival prediction if the influence of bus stops is neglected.

We propose a CTSP method named CTAS, which considers the low penetration of connected vehicles, the widespread application of adaptive signal control, and the influence of bus stops. The main contributions of this research are as follows.

(a) A CTSP method that integrates the benefits of CTSP and adaptive signal control is proposed under an adaptive signal control environment to enhance travel efficiency for passengers and transit vehicles.

(b) A queue prediction model and a distance prediction model are built. The distance between the connected transit vehicle and stop line is predicted with C-V2X technology by considering the influence of bus stops, particularly the impact of multiple connected transit vehicles passing through the same bus stop. A rolling horizon strategy is used to continuously adjust the signal timing plan.

The remainder of this paper is organized as follows. We describe the methodology of the proposed method in Section II. In Section III, we present the results of the experiments and performance analysis, and compare our method with the existing methods. Finally, we summarize the conclusions of this study in Section IV.

II. METHDOLOGY

A. SYSTEM FRAMEWORK

The framework of CTAS is illustrated in Fig. 1. The framework has two key parts: model prediction and optimization. The queue length is predicted according to real-time traffic data and transit vehicle data in the model prediction module. Then, the distance from the transit vehicle to the stop line is predicted according to real-time transit vehicle data, the queue length, location of bus stops, dwell time, and the preceding transit vehicles at the bus stop. The signal timing plan is solved by a genetic algorithm (GA) to minimize total person delay in the optimization module. We make following assumptions for model simplicity.

(a) Only the transit vehicles are connected vehicles that can broadcast information including position, speed, heading angle, number of passengers, and schedule, to the signal control system via V2I communication. The other vehicles are non-connected vehicles. The reliable communication range of V2I is more than 300 meters [28].

(b) The roadside perception system obtains real-time traffic information, such as traffic volume and the number of queued vehicles. The detection range of the roadside perception system is about 200 meters [29].

(c) The bus stop can only accommodate one bus.

Fig. 2 shows the procedure of our proposed method, which consists of three components. (a) The input component acquires traffic data and transit vehicle data from the roadside perception system and connected transit vehicles, respectively. (b) The prediction component predicts the queue length and the distance between the transit vehicle and the stop line according to current traffic volume, queue length, location of transit vehicles, and location of bus stops. (c) The optimization component optimizes the signal timing plan by minimizing the total person delay. Table 1 presents the inputs and outputs of our proposed method.

B. MODEL PREDICTION

1) QUEUE PREDICTION

Queue prediction involves estimating the number of queued vehicles $n_{i,m,t}$ and the queue length $Q_{i,m,t}$ for movement m in phase $i(i = 1,2,3,4)$ at time t within the prediction horizon. The prediction horizon is the sum of durations of all phases. The duration of each phase includes the green duration and amber time. The number of queued vehicles at time t is predicted based on incremental queue accumulation method [30], which takes into account the arrival flow rate $q_{i,m}$, vehicle departure flow rate $r_{i,m,t}$ at time t, and the previous number of vehicles $n_{i,m,t-1}$,

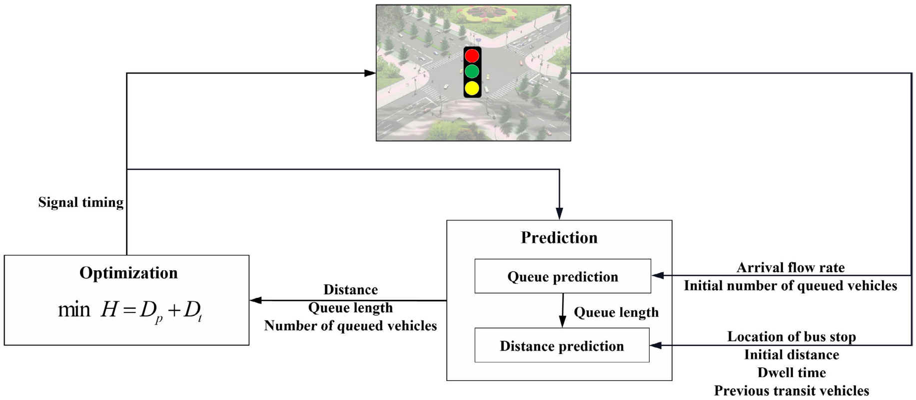

FIGURE 1. The framework of CTAS.

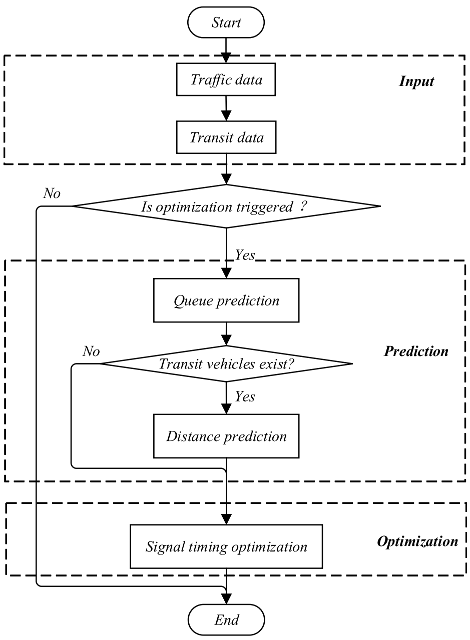

FIGURE 2. The procedure of CTAS.

TABLE 1. Parameters of inputs and outputs.

Type	Symbol	Definition	Source
Inputs	$x_{i,m,j}, y_{i,m,j}$	x-coordinate and y-coordinate of the *j-th* transit vehicle for movement *m* in phase *i*	V2I
	$\theta_{i,m,j}$	Heading angle of the *j-th* transit vehicle for movement *m* in phase *i*	
	$v_{i,m,j}$	Speed of the *j-th* transit vehicle for movement *m* in phase *i*	
	$p^t_{i,m,j}$	Occupancy of the *j-th* transit vehicle for movement m in phase i	
	$T^I_{i,m,j}$	Departure interval of the *j-th* transit vehicle for movement *m* in phase *i*	
	$T^D_{i,m,j}$	Deviation to schedule of the *j-th* transit vehicle for movement *m* in phase *i*	
	$V_{i,m,0}$	Traffic volume for movement *m* in phase *i* during the current detection period	Roadside perception system
	$n_{i,m,0}$	Real-time average queued vehicles in all lanes of movement *m* in phase *i*	
Outputs	g_i	Green duration of phase *i*	

as shown in (1). The queue length $Q_{i,m,t}$ for movement m in phase i is calculated with (2). The arrival flow rate $q_{i,m}$ can be transformed from the traffic volume detected by the roadside perception system as shown in (3). The initial number of queued vehicles $n_{i,m,0}$ is the average number of queued vehicles in all lanes when optimization is triggered. The number of queued vehicles for each lane can be detected by the roadside perception system. The initial traffic volume $V_{i,m,0}$ can also be collected by cameras. The saturation flow rate $s_{i,m}$ can found in reference [31]. The predicted number of queued vehicles $n_{i,m,t}$ and the queue length $Q_{i,m,t}$ at time t, can be inferred with the previous number of queued vehicles at time *t-1*, initial traffic volume $V_{i,m,0}$, and saturation flow rate $s_{i,m}$.

$$n_{i,m,t} = n_{i,m,t-1} + \frac{q_{i,m} - r_{i,m,t}}{l_{i,m}} \Delta t \tag{1}$$

$$Q_{i,m,t} = n_{i,m,t} h_s \tag{2}$$

$$q_{i,m} = \frac{V_{i,m,0}}{t_v} \tag{3}$$

where Δt is time interval, the default is 1 second,

h_s is average space headway of queued vehicles,

$l_{i,m}$ is the number of lanes for movement m in phase i,

$V_{i,m,0}$ is the initial traffic volume for movement m in phase i,

t_v is the sampling interval for traffic volume detection,

$q_{i,m}$ is the arrival flow rate for movement m in phase i.

Vehicle departure flow rate $r_{i,m,t}$ can be calculated with (4). It is related to phase status, the initial number of queued vehicles $n_{i,m,0}$, arrival flow rate $q_{i,m}$, and saturation flow rate $s_{i,m}$ when optimization is triggered. $r_{i,m,t}$ has three cases:

(a) $r_{i,m,t} = 0$, when the phase status at time t is not green.

(b) $r_{i,m,t} = q_{i,m}$, when the phase status at time t is green and the queue has dissipated.

(c) $r_{i,m,t} = s_{i,m}$, when the phase status at time t is green and the queue has not dissipated.

$$r_{i,m,t} = \begin{cases} 0, & t \le t_i^G \; or \; t > t_i^R \\ q_{i,m}, & \left(t - t_i^G\right) s_{i,m} \ge q_{i,m}t + N_{i,m,0} \; and \; t \le t_i^R \\ s_{i,m}, & \left(t - t_i^G\right) s_{i,m} < q_{i,m}t + N_{i,m,0} \; and \; t \le t_i^R \end{cases} \tag{4}$$

$$t_i^G = \sum_{k=1}^{i-1} (g_k + y_k - \gamma_k \tau_k) + \max(0, t_l - \gamma_i \tau_i) \tag{5}$$

$$t_i^R = \sum_{k=1}^{i} (g_k + y_k - \gamma_k \tau_k) \tag{6}$$

$$N_{i,m,0} = n_{i,m,0} l_{i,m} \tag{7}$$

where t_i^G is the start time of effective green time in phase i, t_i^R is the end time of effective green time in phase i, $s_{i,m}$ is saturation flow rate of movement m in phase i, $N_{i,m,0}$ is the total initial number of queued vehicles in all lanes of movement m in phase i, g_k is the green duration of phase k, y_k is the amber time of phase k, γ_k indicates whether phase k is green when the optimization starts, τ_k is the elapsed green time of phase k when the optimization starts, t_l is the lost time when a phase starts, $n_{i,m,0}$ is initial number of queued vehicles for movement m in phase i. $\gamma_k = 1$, if the phase k is green when the optimization starts, otherwise, $\gamma_k = 0$. τ_k is valid only if the phase k is green when the optimization starts, otherwise, $\tau_k = 0$.

2) DISTANCE PREDICTION

We predict the distance between the transit vehicle and the stop line. This distance is used to calculate bus delay. The initial distance $d_{i,m,j,0}$ is determined in RSU by the position of the *j-th* transit vehicle and stop line, as shown in (8). This distance is used to predict the distance between the *j-th* transit vehicle to the stop line within the prediction horizon.

$$d_{i,m,j,0} = \sqrt{\left(x_{i,m,j} - x_{i,m}^s\right)^2 + \left(y_{i,m,j} - y_{i,m}^s\right)^2} \tag{8}$$

where $x_{i,m}^s$ and $y_{i,m}^s$ are the x and y coordinate of the center point of the stop line corresponding to movement m in phase i, respectively. There are two scenarios when predicting distance between the transit vehicle and the stop line.

Scenario 1: There are no other transit vehicles between the *j-th* transit vehicle and the bus stop. Therefore, the *j-th* transit vehicle is not affected by the preceding transit vehicles when entering the bus stop. Fig. 3 shows the situation of the transit vehicle not encountering a queue, encountering the queue after leaving the bus stop, encountering the queue at the bus stop, and encountering the queue before arriving at the bus stop, respectively. Fig. 3(b) illustrates that the transit vehicle stays at the bus stop from time $t_{i,m,j}^s$ to time $t_{i,m,j}^d$, and then encounters the queue at time t_q. Fig. 3(c) shows the transit vehicle has to stay at the bus stop even it has finished passenger service at time $t_{i,m,j}^d$, because the queue extends beyond the bus stop. Fig. 3(d) presents that the transit vehicle encounters the queue at time t_q, and subsequently arrives at the bus stop at time $t_{i,m,j}^s$ until the queue dissipates. The predicted distance $d_{i,m,j,t}$ at time t can be calculated with (9)–(13), as shown at the bottom of the next page. With C-V2X technology, we can obtain the location of the bus stop and calculate the real-time distance between the transit vehicle and the bus stop. As shown in (11) and (12), the dwell time of the transit vehicle at the bus stop is considered, which enhances the accuracy of the distance prediction for the *j-th* transit vehicle.

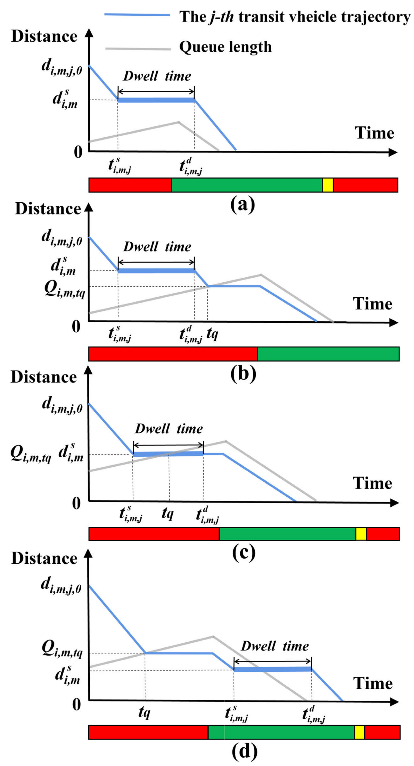

FIGURE 3. Queue length and distance between transit vehicle to stop line over time for scenario 1. (a) no queues encountered. (b) encountering the queue after leaving bus stop, (c) encountering the queue at bus stop, (d) encountering the queue before arriving bus stop.

Scenario 2: There are other transit vehicles between the *j-th* transit vehicle and the bus stop. Therefore, the *j-th* transit vehicle is prevented from entering the bus stop by preceding transit vehicles. Fig. 4 shows the situation of the transit vehicle not encountering a queue, encountering the queue after leaving the bus stop, encountering the queue at the bus stop, and encountering the queue before arriving at the bus stop, respectively. The predicted distance $d_{i,m,j,t}$ at time t can be calculated with (9), (12), and (13). With C-V2X technology, the real-time data of the *j-th* transit vehicle and its preceding transit vehicles can be obtained. The distance prediction for *j-th* transit vehicle can be more accurate by considering the influence of preceding transit vehicles at the bus stop.

where

$v_{i,m,j}$ is the default speed of the transit vehicle,

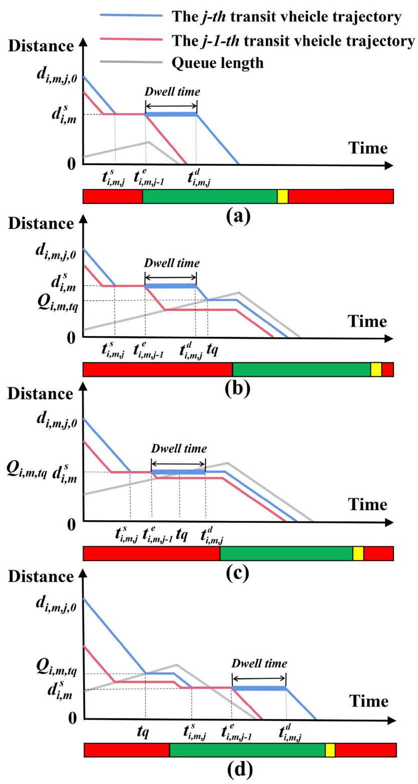

FIGURE 4. Queue length and distance between transit vehicle to stop line over time for scenario 2. (a) no queues encountered. (b) encountering the queue after leaving bus stop, (c) encountering the queue at bus stop, (d) encountering the queue before arriving bus stop.

Δt is time interval, the default is 1 second,

$d^s_{i,m}$ denotes the distance between the bus stop and stop line for movement m in phase i,

$Q_{i,m,t-1}$ denotes the queue length at time $t-1$,

h_s is the average space headway,

$t^s_{i,m,j}$ denotes the time when transit vehicle arrives the bus stop,

$t^d_{i,m,j}$ denotes the time when transit vehicle completes the boarding service,

T_l is the lost time of transit vehicle entering and exiting the bus stop,

q_p is the passenger arrival rate at the bus stop,

T_s is the average time required for a passenger to board a bus,

$t^e_{i,m,j-1}$ denotes the time when the j-1-th transit vehicle exits the bus stop,

$r_{i,m,t}$ is vehicle departure flow rate for movement m in phase i at time t,

$T^I_{i,m,j}$ is departure interval of the j-th transit vehicle for movement m in phase i,

$T^D_{i,m,j}$ is the deviation to schedule of the j-th transit vehicle for movement m in phase i.

$t^s_{i,\mathrm{m},j}$ and $t^d_{i,m,j}$ are calculated only when the bus stop is located between transit vehicle and stop line. T_s is assumed to be a constant. Therefore, the dwell time of a transit vehicle is directly proportional to the number of passengers boarding the bus.

C. OPTIMIZATION

The optimization aims to minimize the total person delay at the intersection during the prediction horizon. The total person delay is the sum of the passenger delay for private vehicles and the weighted passenger delay for transit vehicles. Based on the predicted queue length and the predicted distance between the transit vehicles and stop line, we can determine whether the transit vehicles and private vehicles are delayed. The objective function H is designed to obtain

$$d_{i,m,j,t} = \begin{cases} \max(d_{i,m,j,t-1} - v_{i,m,j}\Delta t, d^s_{i,m}), & d_{i,m,j,t-1} > d^s_{i,m} \text{ and } d_{i,m,j,t-1} > Q_{i,m,t-1} \\ \max(d_{i,m,j,t-1} - r_{i,m,t}h_s\Delta t, d^s_{i,m}), & d_{i,m,j,t-1} > d^s_{i,m} \text{ and } d_{i,m,j,t-1} \le Q_{i,m,t-1} \\ d^s_{i,m}, & t \ge t^s_{i,m,j} \text{ and } t < t^d_{i,m,j} \\ d_{i,m,j,t-1} - v_{i,m,j}\Delta t, & t \ge t^d_{i,m,j} \text{ and } d_{i,m,j,t-1} > Q_{i,m,t-1} \\ d_{i,m,j,t-1} - r_{i,m,t}h_s\Delta t, & t \ge t^d_{i,m,j} \text{ and } d_{i,m,j,t-1} \le Q_{i,m,t-1} \end{cases} \tag{9}$$

$$t^s_{i,m,j} = \begin{cases} 0, & d_{i,m,j,0} < d^s_{i,m} or d_{i,m,j,t} > d^s_{i,m} \\ t, & d_{i,m,j,t-1} > Q_{i,m,j,t-1} \text{ and } d_{i,m,j,t-1} > d^s_{i,m} \text{ and } d_{i,m,j,t-1} - v_{i,m,j}\Delta t \le d^s_{i,m} \\ t, & d_{i,m,j,t-1} \le Q_{i,m,j,t-1} \text{ and } d_{i,m,j,t-1} > d^s_{i,m} \text{ and } d_{i,m,j,t-1} - r_{i,m,t}h_s\Delta t \le d^s_{i,m} \end{cases} \tag{10}$$

$$t^d_{i,m,j} = \begin{cases} t^s_{i,m,j} + T_l + q_p(T^I_{i,m,j} + T^D_{i,m,j})T_s, & d_{i,m,j,0} \ge d^s_{i,m} \\ 0, & d_{i,m,j,0} < d^s_{i,m} \end{cases} \tag{11}$$

$$t^d_{i,m,j} = \begin{cases} \max(t^s_{i,m,j}, t^e_{i,m,j-1}) + T_l + q_p(T^I_{i,m,j} + T^D_{i,m,j})T_s, & d_{i,m,j,0} \ge d^s_{i,m} \\ 0, & d_{i,m,j,0} < d^s_{i,m} \end{cases} \tag{12}$$

$$t^e_{i,m,j-1} = \begin{cases} 0, & d_{i,m,j-1,0} < d^s_{i,m} or d_{i,m,j-1,t} > d^s_{i,m} \\ t^d_{i,m,j-1}, & t \ge t^s_{i,m,j-1} \text{ and } t \le t^d_{i,m,j-1} \\ t, & t > t^d_{i,m,j-1} \text{ and } d_{i,m,j-1,t-1} = d^s_{i,m} \end{cases} \tag{13}$$

the green duration g_i for each phase.

$$\min H = D_p + D_t$$
$$s.t. \begin{cases} g_i^{\min} \leq g_i \leq g_i^{\max} \\ g_i \in N^* \\ g_i * s_{i,m} >= q_{i,m} t_i^G + N_{i,m,0} \end{cases} \tag{14}$$

where D_p is the total private vehicle passenger delay, D_t is the total weighted transit passenger delay, $s_{i,m}$ is the saturation flow rate for movement m in phase i, $q_{i,m}$ is the arrival flow rate for movement m in phase i, $N_{i,m,0}$ is the initial number of queued vehicles in all lanes of movement m for phase i, g_i is the green duration of phase i, t_i^G is the start time of effective green time for phase i, g_i^{min} and g_i^{max} are the lower limit and upper limit of green duration of phase i, respectively. We consider the following constraints: (a) The green duration for all phases must be a positive integer and should be within the lower and upper bounds. (b)Sufficient green time is allocated for each phase to prevent vehicles from queuing again. The delay for private vehicles depends on the predicted number of queued vehicles during the prediction horizon. The passenger delay for private vehicle D_p is calculated as follows.

$$D_p = \sum_{t=1}^{T} \sum_{i=1}^{I} \sum_{m=1}^{M_i} p_p l_{i,m} n_{i,m,t} \tag{15}$$
$$T = \sum_{i=1}^{I} (g_i + y_i - \gamma_i \tau_i) \tag{16}$$

where p_p is the average private vehicle occupancy, $l_{i,m}$ is the number of lanes for movement m in phase i, M_i is the number of movements in phase i, I is the number of phases, T is the sum of the durations of all phases. The delay for transit vehicles depends on the predicted queue length and the distance between the transit vehicle and the stop line [23]. The weighted transit passenger delay D_t for transit vehicles is calculated with (17), (18), and (19).

$$D_t = \sum_{t=1}^{T} \sum_{i=1}^{I} \sum_{m=1}^{M_i} \sum_{j=1}^{J_{i,m}} \left(w_{i,m,j} p_{i,m,j}^t d_{i,m,j,t}^T \right) \tag{17}$$
$$d_{i,m,j,t}^T = \begin{cases} 0, & d_{i,m,j,t} > Q_{i,m,t} \text{ or } d_{i,m,j,t} < 0 \\ 1, & d_{i,m,j,t} \leq Q_{i,m,t} \end{cases} \tag{18}$$
$$w_{i,m,j} = \begin{cases} \min\left(w_{\min} + \dfrac{T_{i,m,j}^D}{T_a}, \ w_{\max} \right), T_{i,m,j}^D > 0 \\ w_{\min}, \quad T_{i,m,j}^D \leq 0 \end{cases} \tag{19}$$

where

$w_{i,m,j}$ is the weight,

$p_{i,m,j}^t$ is the occupancy of the j-th transit vehicle for movement m in phase i,

$d_{i,j,m,t}^T$ indicates whether the j-th transit vehicle for movement m in phase i is delayed or not at time t,

$T_{i,m,j}^D$ is the deviation to schedule of the j-th transit vehicle for movement m in phase i,

T_a is the acceptable deviation,

$J_{i,m}$ is the number of transit vehicles for phase i,

w_{min} and w_{max} are the lower and upper bounds of weight, respectively.

The genetic algorithm (GA), which is a global search method, is used to obtain the optimal signal timing plan [33]. The parameters of GA are shown in Table 2.

TABLE 2. Parameters of GA.

Parameters	Value
Population size	50
Max generations	500
Fitness function	1/H
Select function	Roulette wheel selection
Crossover probability	0.8
Mutation probability	0.2

D. ROLLING HORIZON STRATEGY

The rolling horizon strategy is used to continuously adjust the signal timing plan according to changing traffic conditions. Fig. 5 illustrates two ways to initiate the optimization process. t_{k-1} and t_k represent the start time of the last optimization procedure and current optimization procedure, respectively. In Fig. 5(a), no transit vehicles are detected during the default rolling window T_r. The next optimization procedure will start at the amber time after the rolling window. Fig. 5(b) illustrates that a transit vehicle is detected at time t_k. The next optimization procedure is triggered immediately. The green duration of four phases is calculated in each optimization procedure.

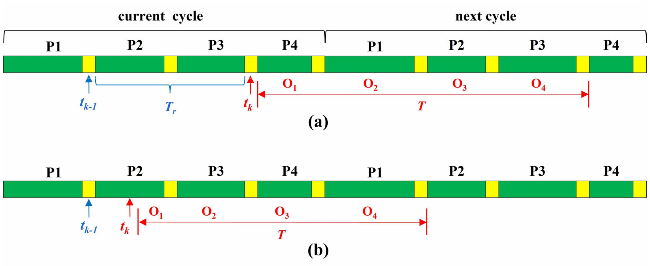

FIGURE 5. Two ways to trigger an optimization procedure. (a) No transit vehicles are detected, (b) A transit vehicle is detected.

III. EXPERIMENTS AND EVALUATION

A. EXPERIMENT

The proposed method is verified using measured data from the Fenglin-pingchuan intersection in Changsha, China, as shown in Fig. 6(a). Actual traffic data are obtained from the roadside perception system. The roadside perception system consists of four cameras, a roadside unit (RSU), and an edge computing unit (ECU), as shown in Fig. 6. Cameras are installed on the different roadside traffic crossbars to detect the vehicles driving on the road. The RSU can communicate with the connected transit vehicles through V2I

TABLE 3. Comparison between CTAS, L-TSP, PACT, and CTA when one bus arrives.

	L-TSP	PACT	CTA	CTAS	CTAS vs.L-TSP	CTAS vs.PACT	CTAS vs.CTA
Bus delay(s)	75.23	65.83	67.23	**42.23**	-43.86%	-35.85%	-37.18%
Private vehicle delay(s)	37.19	36.08	**35.90**	36.12	-2.89%	0.11%	0.60%
Person delay (s)	41.28	37.80	37.71	**36.48**	-11.63%	-3.48%	-3.25%

TABLE 4. Comparison between CTAS, L-TSP, PACT, and CTA when two buses arrive.

	L-TSP	PACT	CTA	CTAS	CTAS vs.L-TSP	CTAS vs.PACT	CTAS vs.CTA
Bus delay(s)	79.90	69.80	64.40	**48.90**	-38.80%	-29.94%	-24.07%
Private vehicle delay(s)	41.91	33.08	**32.77**	33.63	-19.77%	1.66%	2.61%
Person delay (s)	45.85	36.60	35.90	**35.10**	-23.44%	-4.10%	-2.22%

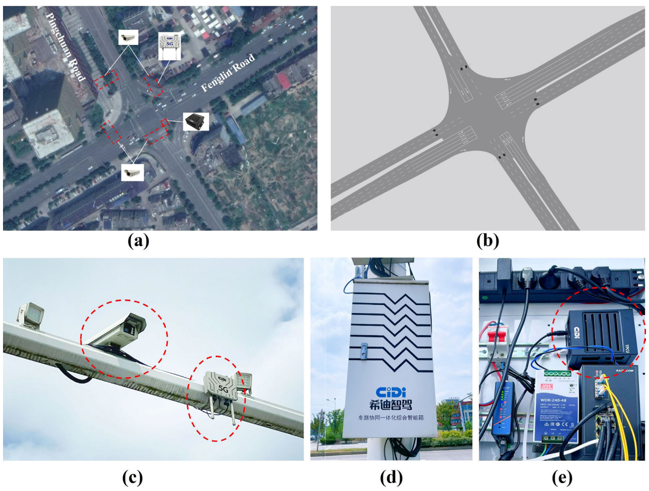

FIGURE 6. Experimental scenario. (a) Fenglin-pingchuan intersection, (b) Road network model, (c) Camera and RSU, (d) Pole box, (e) ECU.

communication. A road network model, which is the same with the Fenglin-pingchuan intersection, is constructed in a microscopic traffic simulation software.

We studied the influence of bus stops by placed a bus stop within 200 meters upstream of the intersection on the west approach. Different bus lines are designed to evaluate the influence of multiple buses approaching the same bus stop. The departure interval of each bus line is determined based on actual transit data obtained by RSU via V2I communication. The traffic volume for each movement is measured during different periods from the test site.

The cycle of the background signal timing plan is 110 seconds. The occupancy of each private vehicle and bus is set as 1 passenger and 30 passengers, respectively. The average time for a passenger to board a bus is 2 seconds. The lost time of a bus entering and exiting the bus stop is 8 seconds. The total traffic volume is set as 4109 pcu/h and the V/C ratio is 0.8.

Three different methods are used to compare with our proposed method.

1) L-TSP [24]. It is a cooperative transit signal priority method under fixed-time signal control. This method considers the influence of bus stops in the process of transit arrival prediction. It achieves transit signal priority by minimizing the sum of bus delay and signal timing deviation.
2) PACT [28]. It is a cooperative transit signal priority method under adaptive signal control. This method optimizes signal timing plan to minimize the total person delay. However, this method does not consider the influence of bus stops.
3) CTA. Similar to CTAS, CTA also optimizes the signal timing plan to minimize the total person delay. However, it does not consider the influence of bus stops compared with CTAS.

B. EVALUATION

The bus delay, private vehicle delay, and person delay are used to evaluate these methods. We evaluated the influence of the different numbers of transit vehicles approaching the same bus stop from the west approach, including scenarios of one bus, two buses, and three buses. Table 3, Table 4, and Table 5 present the evaluation results of these scenarios. As shown in the tables, CTAS achieves the best performance in terms of bus delay and person delay. L-TSP achieves the worst performance. L-TSP only adjusts the signal timing plan upon bus arrival, while the other methods continuously adjust the signal timing plan according to traffic conditions. In the scenario of one bus, CTAS can reduce bus delay by 43.9%/35.9%/37.2% compared with L-TSP/PACT/CTA. It also can reduce the person delay by 11.6%/3.5%/3.3% compared with L-TSP/PACT/CTA. Compared with CTA, CTAS considers the impact of the dwell time at the bus stop during bus arrival prediction. Therefore, it can allocate sufficient green time to allow the bus to pass through the intersection.

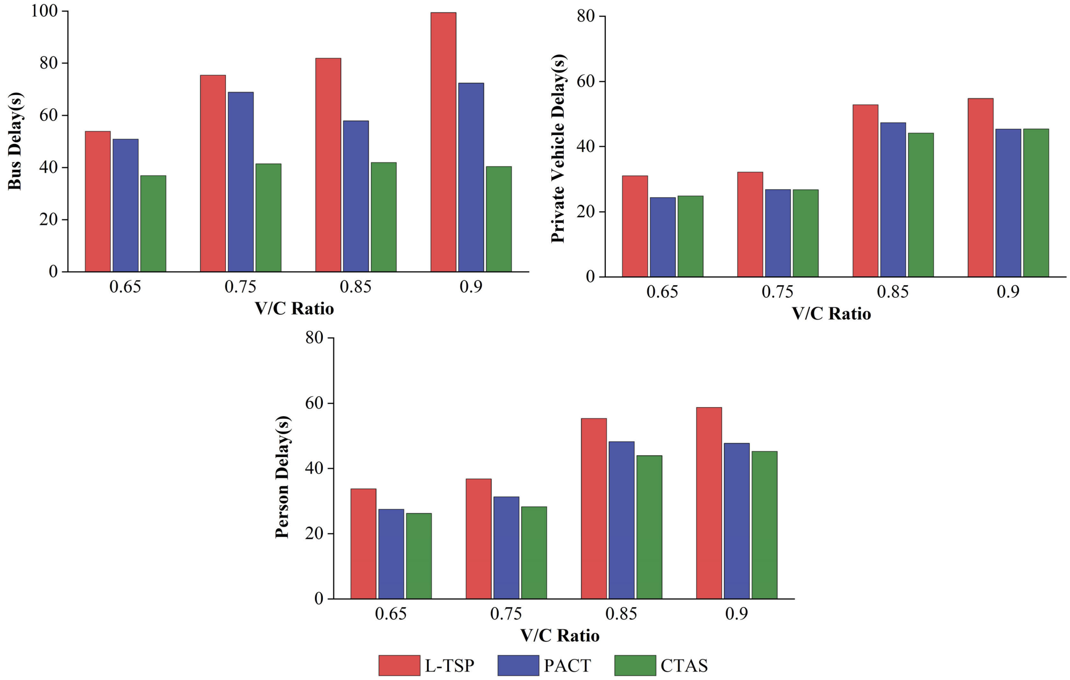

FIGURE 7. Delay under different V/C ratio. (a) Bus delay, (b) Private vehicle delay, (c) Person delay.

TABLE 5. Comparison between CTAS, L-TSP, PACT, and CTA when three buses arrive.

	L-TSP	PACT	CTA	CTAS	CTAS vs.L-TSP	CTAS vs.PACT	CTAS vs.CTA
Bus delay(s)	87.76	61.76	54.76	**47.76**	-45.58%	-22.67%	-12.78%
Private vehicle delay(s)	41.06	33.31	**33.09**	33.40	-18.66%	0.26%	0.94%
Person delay (s)	47.55	37.16	36.04	**35.39**	-25.58%	-4.77%	-1.82%

CTA, which integrates CTSP and adaptive signal control, achieves better performance than PACT in terms of bus delay, private vehicle delay, and person delay in the scenarios of two buses and three buses. It means CAT can more effectively combine the advantages of CTSP and adaptive signal control than PACT. In the scenarios of two buses and three buses, CTAS shows better performance than CTA in terms of bus delay and person delay. Because CTAS considers the impact of the dwell time of the transit vehicles at the bus stop and multiple transit vehicles approaching the same bus stop. The private vehicle delay of CTAS is slightly larger than that of CTA. It indicates that CTAS reduces delays for transit vehicles without causing many negative impacts on private vehicles.

C. SENSITIVITY ANALYSIS ON CONGESTION LEVELS

Sensitivity analysis is conducted to compare the performance of CTAS, L-TSP, and PACT under different traffic flow conditions. Four sets of traffic flow are set to indicate different traffic congestion levels in a day. The cycle time is calculated using the Webster method. The detailed traffic parameters are shown in Table 6. The scenario of two buses is chosen to evaluate the performance of our method.

TABLE 6. Traffic parameters.

Period	Volume (pcu/h)	V/C ratio	Cycle (s)
19:00~20:00	3410	0.65	70
9:00~10:00	3867	0.75	95
18:00~19:00	4359	0.85	140
8:00~9:00	4611	0.9	170

The comparative results are shown in Fig. 7 and Table 7. Under different traffic flow conditions, CTAS can significantly improve the traffic efficiency of the intersection compared with L-TSP and PACT. Compared with L-TSP, CATS reduces bus delay by 31.54%-59.36%, reduces private vehicle delay by 16.35%-20.02%, and reduces person delay by 20.63%-23.07%. Compared with PACT, CATS reduces bus delay by 27.50%-44.20% and reduces person delay by 4.54%-9.69%.

TABLE 7. Comparative results under different V/C ratio.

	Methods	V/C ratio			
		0.65	0.75	0.85	0.9
Bus delay(s)	L-TSP	53.90	75.40	81.90	99.40
	PACT	50.90	68.90	57.90	72.40
	CTAS	**36.90**	**41.40**	**41.90**	**40.40**
	CTAS vs.L-TSP	-31.54%	-45.09%	-48.84%	-59.36%
	CTAS vs.PACT	-27.50%	-39.91%	-27.63%	-44.20%
Private vehicle delay(s)	L-TSP	31.05	32.16	52.79	54.74
	PACT	**24.35**	26.80	47.31	**45.39**
	CTAS	24.84	**26.73**	**44.16**	45.42
	CTAS vs.L-TSP	-20.02%	-16.89%	-16.35%	-17.02%
	CTAS vs.PACT	1.99%	-0.28%	-6.67%	0.08%
Person delay (s)	L-TSP	33.76	36.78	55.39	58.76
	PACT	27.50	31.33	48.26	47.73
	CTAS	**26.25**	**28.29**	**43.96**	**45.27**
	CTAS vs.L-TSP	-22.24%	-23.07%	-20.63%	-22.95%
	CTAS vs.PACT	-4.54%	-9.69%	-8.91%	-5.15%

IV. CONCLUSION

In this research, we proposed a method that combines the advantages of CTSP and adaptive signal control. Real-time traffic data and transit vehicles data are acquired with the roadside perception system and V2I communication, respectively. Then, we built a queue prediction model and a distance prediction model to compute the delay of vehicles and passengers. We considered the impact of the bus stop to obtain a more accurate bus arrival prediction. The genetic algorithm is used to obtain the signal timing plan to minimize the total person delay. Furthermore, we employed the rolling horizon strategy to continuously adjust the signal timing plan according to changing traffic conditions. The performance of the proposed method is demonstrated using the measured data from the Fenglin-pingchuan intersection. CTAS achieves the best performance in terms of bus delay and person delay under different scenarios, including scenarios of one bus, two buses, and three buses. The results demonstrate that our method outperforms L-TSP and PACT under different traffic congestion levels. Compared with L-TSP/PACT, CATS achieves 31.54%-59.36%/27.50%-44.20% reduction in bus delay and 20.63%-23.07%/4.54%-9.69% reduction in person delay.

Our research could be extended in the following aspects. (a) We only integrate adaptive timing control and CTSP at an isolated intersection. It is important to combine adaptive signal control and TSP in a traffic corridor in the future. (b) We assume that the transit vehicle will drive at a fixed speed in the distance prediction process. However, it is difficult to maintain a constant speed while driving on the actual road. The impact of different speeds on distance prediction for transit vehicles will be explored in future research. (c) The detection range of the roadside perception system is limited, estimating queue length when queue is beyond the range of detection will be studied.

ACKNOWLEDGMENT

The authors would like to thank Liuzhou Dongke Smart City Investment and Development Company Ltd., Management Committee of Hunan Xiang Jiang New Area, and City Traffic Police of Changsha to provide the opportunity and site access for them to do this research.

REFERENCES

[1] A. Shalaby, W. X. Hu, M. Corby, A. Wong, and D. Zhou, "Transit signal priority: Research and practice review and future needs," in *Handbook of Public Transport Research*, Cheltenham, U.K.: Edward Elgar, 2021, ch. 16, pp. 340–372.

[2] M. S. Ali, A. E. Kitali, J. Kodi, P. Alluri, and T. Sando, "Quantifying the safety benefits of transit signal priority using full Bayes before-after study," *J. Transp. Eng., A, Syst.*, vol. 148, no. 1, Jan. 2022, Art. no. 04021102.

[3] Y. Ren, J. Zhao, and X. Zhou, "Optimal design of scheduling for bus rapid transit by combining with passive signal priority control," *Int. J. Sustain. Transp.*, vol. 15, no. 5, pp. 407–418, Mar. 2021.

[4] J. Wang, Y. Han, and J. Zhao, "Conditional transit signal priority optimization at stop-to-stop segments to improve BRT on-time performance," *IEEE Access*, vol. 10, pp. 33512–33526, 2022.

[5] L. T. Truong, G. Currie, M. Wallace, C. De Gruyter, and K. An, "Coordinated transit signal priority model considering stochastic bus arrival time," *IEEE Trans. Intell. Transp. Syst.*, vol. 20, no. 4, pp. 1269–1277, Apr. 2019.

[6] J. Lee, A. Shalaby, J. Greenough, M. Bowie, and S. Hung, "Advanced transit signal priority control with online microsimulation-based transit prediction model," *Transp. Res. Rec., J. Transp. Res. Board*, vol. 1925, no. 1, pp. 185–194, Jan. 2005.

[7] H. M. Abdelghaffar, K. Ahn, and H. A. Rakha, "Developing an adaptive connected vehicle transit signal priority control system," in *Proc. IEEE 23rd Int. Conf. Intell. Transp. Syst. (ITSC)*, Sep. 2020, pp. 1–6.

[8] M. H. Sheffield, G. G. Schultz, D. Bassett, and D. L. Eggett, "Sensitivity analysis of the transit signal priority requesting threshold and the impact on bus performance and general traffic," *Transp. Res. Rec.*, vol. 2675, no. 5, pp. 149–163, May 2021.

[9] K. N. Balke, C. L. Dudek, and T. Urbanik, "Development and evaluation of intelligent bus priority concept," *Transp. Res. Rec., J. Transp. Res. Board*, vol. 1727, no. 1, pp. 12–19, Jan. 2000.
[10] W. Ekeila, T. Sayed, and M. E. Esawey, "Development of dynamic transit signal priority strategy," *Transp. Res. Rec., J. Transp. Res. Board*, vol. 2111, no. 1, pp. 1–9, Jan. 2009.
[11] J. Hu, B. Park, and A. E. Parkany, "Transit signal priority with connected vehicle technology," *Transp. Res. Rec., J. Transp. Res. Board*, vol. 2418, no. 1, pp. 20–29, Jan. 2014.
[12] D. Yang, K. Jiang, D. Zhao, C. Yu, Z. Cao, S. Xie, Z. Xiao, X. Jiao, S. Wang, and K. Zhang, "Intelligent and connected vehicles: Current status and future perspectives," *Sci. China Technological Sci.*, vol. 61, no. 10, pp. 1446–1471, Oct. 2018.
[13] M. Steadman and B. Huntsman, "Connected vehicle infrastructure: Deployment and funding overview," Texas A&M Transp. Inst., TX, USA, Tech. Rep., PRC 17-77 F, Jan. 2018.
[14] J. Li, L. Peng, and T. Z. Qiu, "Real-time predictive coordination based on vehicle-triggered platoon dispersion in a low penetration connected vehicle environment," *IET Intell. Transp. Syst.*, vol. 15, no. 12, pp. 1548–1561, Dec. 2021.
[15] Z. Cvijovic, M. Zlatkovic, A. Stevanovic, and Y. Song, "Conditional transit signal priority for connected transit vehicles," *Transp. Res. Rec., J. Transp. Res. Board*, vol. 2676, no. 2, pp. 490–503, Feb. 2022.
[16] J. Li, C. Qiu, L. Peng, and T. Z. Qiu, "Signal priority request delay modeling and mitigation for emergency vehicles in connected vehicle environment," *Transp. Res. Rec., J. Transp. Res. Board*, vol. 2672, no. 18, pp. 45–57, Dec. 2018.
[17] K. Yang, M. Menendez, and S. I. Guler, "Implementing transit signal priority in a connected vehicle environment with and without bus stops," *Transportmetrica B, Transp. Dyn.*, vol. 7, no. 1, pp. 423–445, Dec. 2019.
[18] J. Hu, B. B. Park, and Y.-J. Lee, "Transit signal priority accommodating conflicting requests under connected vehicles technology," *Transp. Res. C, Emerg. Technol.*, vol. 69, pp. 173–192, Aug. 2016.
[19] X. Zeng, X. Sun, Y. Zhang, and L. Quadrifoglio, "Person-based adaptive priority signal control with connected-vehicle information," *Transp. Res. Rec., J. Transp. Res. Board*, vol. 2487, no. 1, pp. 78–87, Jan. 2015.
[20] S. Xianmin, Y. Mili, L. Di, and M. Lin, "Optimization method for transit signal priority considering multirequest under connected vehicle environment," *J. Adv. Transp.*, vol. 2018, pp. 1–10, Jun. 2018.
[21] J. Zhao and X. Zhou, "Improving the operational efficiency of buses with dynamic use of exclusive bus lane at isolated intersections," *IEEE Trans. Intell. Transp. Syst.*, vol. 20, no. 2, pp. 642–653, Feb. 2019.
[22] J. E. Siegel, D. C. Erb, and S. E. Sarma, "A survey of the connected vehicle landscape—Architectures, enabling technologies, applications, and development areas," *IEEE Trans. Intell. Transp. Syst.*, vol. 19, no. 8, pp. 2391–2406, Aug. 2018.
[23] X. Zeng, Y. Zhang, K. N. Balke, and K. Yin, "A real-time transit signal priority control model considering stochastic bus arrival time," *IEEE Trans. Intell. Transp. Syst.*, vol. 15, no. 4, pp. 1657–1666, Aug. 2014.
[24] X. Zeng, Y. Zhang, J. Jiao, and K. Yin, "Route-based transit signal priority using connected vehicle technology to promote bus schedule adherence," *IEEE Trans. Intell. Transp. Syst.*, vol. 22, no. 2, pp. 1174–1184, Feb. 2021.
[25] S. Liang, R. Leng, H. Zhang, and J. Zhao, "Two-stage transit signal priority control method to improve reliability of bus operation considering stochastic process," *Transp. Res. Rec., J. Transp. Res. Board*, vol. 2677, no. 2, pp. 1713–1727, Feb. 2023.
[26] G. Liu and T. Z. Qiu, "Trade-offs between bus and private vehicle delays at signalized intersections: Case study of a multiobjective model," *Transp. Res. Rec., J. Transp. Res. Board*, vol. 2539, no. 1, pp. 72–83, Jan. 2016.
[27] W.-H. Lee and C.-Y. Chiu, "Design and implementation of a smart traffic signal control system for smart city applications," *Sensors*, vol. 20, no. 2, p. 508, Jan. 2020.
[28] W.-H. Lee and H.-C. Wang, "A person-based adaptive traffic signal control method with cooperative transit signal priority," *J. Adv. Transp.*, vol. 2022, pp. 1–17, Mar. 2022.
[29] J. I. Engel, J. Martín, and R. Barco, "A low-complexity vision-based system for real-time traffic monitoring," *IEEE Trans. Intell. Transp. Syst.*, vol. 18, no. 5, pp. 1279–1288, May 2017.
[30] D. W. Strong, N. R. Rouphail, and K. Courage, "New calculation method for existing and extended HCM delay estimation procedure," in *Proc. 87th Annu. Meeting Transp. Res. Board*, Washington, DC, USA, 2006, pp. 1–20.
[31] Transportation Research Board, *Highway Capacity Manual*, 5th ed., Washington, DC, USA, 2010, pp. 4–12.
[32] Y. Feng, K. L. Head, S. Khoshmagham, and M. Zamanipour, "A real-time adaptive signal control in a connected vehicle environment," *Transp. Res. C, Emerg. Technol.*, vol. 55, pp. 460–473, Jun. 2015.
[33] S. Katoch, S. S. Chauhan, and V. Kumar, "A review on genetic algorithm: Past, present, and future," *Multimedia Tools Appl.*, vol. 80, no. 5, pp. 8091–8126, Feb. 2021.

CHANGLONG ZHANG received the Ph.D. degree in information and communication engineering from the National University of Defense Technology, China, in 2004. He is currently an Associate Professor with Changsha Intelligent Driving Institute Company Ltd. His current research interests include V2X, connected vehicles, and cooperative ITS.

XIAODONG YANG received the B.S. and M.S. degrees in traffic and transportation engineering from the Changsha University of Science and Technology, Changsha, China, in 2016 and 2019, respectively. He is currently an Algorithm Engineer with Changsha Intelligent Driving Institute Company Ltd. His research interests include C-ITS, traffic flow theory, traffic signal control, and transit signal priority.

JIMIN WEI received the M.S. degree in control science and engineering from Central South University, China, in 2013. He is currently a Senior Engineer with Changsha Intelligent Driving Institute Company Ltd. His current research interests include sensor calibration, multi-sensor fusion, V2X, C-ITS, and artificial intelligence.

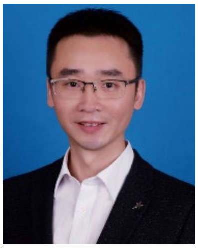

SHUO YANG graduated from Guangxi University, in 2002. He is currently the Chairperson and the General Manager of Liuzhou Dongke Smart City Investment and Development Company Ltd. His current research interests include intelligent city, V2X, big data, industrial internet, and intelligent traffic systems.

JINGANG DAI received the master's degree in mechanical engineering from Ningbo University, China, in 2016. He is currently a Senior Engineer with Changsha Intelligent Driving Institute Company Ltd. His current research interests include sensor calibration and V2X.

SHIBO QU received the M.S. degree in electronic science and technology from Hunan University, in 2013. He is currently the Deputy Technical Director of V2X and Cooperative ITS of Changsha Intelligent Driving Institute Company Ltd. His current research interests include V2X communication, the development scenarios of connected vehicle, and intelligent traffic systems.